CrossMark

RESEARCH PAPER

Toxicity of silver nanoparticles against bacteria, yeast, and algae

**Loredana S. Dorobantu · Clara Fallone ·
Adam J. Noble · Jonathan Veinot · Guibin Ma ·
Greg G. Goss · Robert E. Burrell**

Abstract The toxicity mechanism employed by silver nanoparticles against microorganisms has captivated scientists for nearly a decade and remains a debatable issue. The question most frequently asked is whether silver nanoparticles exert specific effects on microorganisms beyond the well-documented antimicrobial activity of Ag^+. Here, we study the effects of citrate- (d = 17.5 ± 9.4 nm) and 11-mercaptoundecanoic acid (d = 38.8 ± 3.6 nm)-capped silver nanoparticles on microorganisms belonging to various genera. The antimicrobial effect of Ag^+ was distinguished from that of nanosilver by monitoring microbial growth in the presence and absence of nanoparticles and by careful comparison of the responses of equimolar silver nitrate solution. The results show that when using equimolar silver solutions, silver nitrate has higher toxic potential on all microorganisms than both nanoparticles tested. Furthermore, some microorganisms are more susceptible to silver than others and the choice of capping agent is relevant in the toxicity. Atomic force microscopy disclosed that $AgNO_3$ had a destructive effect on algae. The antimicrobial activity of nanosilver could be exploited to prevent microbial colonization of medical devices and to determine the fate of nanoparticles in the environment.

L. S. Dorobantu (✉) · C. Fallone
Department of Chemical and Materials Engineering, University of Alberta, Edmonton, AB T6G 2V4, Canada
e-mail: loredana@ualberta.ca

A. J. Noble
Department of Biology, Trent University, Peterborough, ON K9J 7B8, Canada

J. Veinot · G. Ma
Department of Chemistry, University of Alberta, Edmonton, AB T6G 2G2, Canada

G. G. Goss
Department of Biological Sciences, University of Alberta, Edmonton, AB T6G 2E9, Canada

R. E. Burrell
Department of Biomedical Engineering, University of Alberta, Edmonton, AB T6G 2V2, Canada

Introduction

Following the discovery of the atomic force microscope (AFM) by Binnig et al. in 1986, nanotechnology has evolved to produce a variety of nanomaterials with significant potential impact on optimizing manufacturing processes, revolutionizing the treatment of illnesses and patient care products, as well as

remediating polluted environments (Pace et al. 2010; MacCormack and Goss 2008).

A large number of nanomaterials presently used in consumer products are metal-based nanoparticles including Ag, Cu, Ti, Zn, and Au. Owing to their large surface area:volume ratio and high reactivity compared to the bulk solids, nanosized metal particles exhibit remarkable physical, chemical, and biological properties (Nel et al. 2006; Fubini et al. 2011). The unique properties of metal nanoparticles confer on them high reactivity and allow their successful application in research and development (Schacht et al. 2013).

Silver nanoparticles (AgNPs) are among the most widely used metallic nanoparticles due to their unique physicochemical characteristics such as optical, electrical and biological properties, strong broad-spectrum antimicrobial and anti-inflammatory activity, as well as relatively low manufacturing cost. All of these properties confer on them major advantages for the development of alternative products. The Woodrow Wilson database currently lists over 300 consumer products that contain AgNPs, including clothing, personal care products, washing machines, refrigerators, electronics, and medical devices like catheters, implant surfaces, wound dressings, and plasters (Kittler et al. 2010).

Even though the incorporation of AgNPs in consumer products has increased substantially in recent years, their toxic effects have not been studied extensively (Martinez-Gutierrez et al. 2012). Regulatory agencies around the world monitor nanoparticles fate prompting research for a detailed understanding of their toxicity (Maurer-Jones et al. 2013). Notably, it is of paramount importance to determine if the toxic effects are attributable to nanoparticles themselves or ionic metal dissociating from their surface.

Although the biocidal impact of Ag^+ on microorganisms is well-documented, the mechanism by which AgNPs exert their bioactivity is not fully elucidated (Martinez-Gutierrez et al. 2012; Navarro et al. 2008). Evidence has shown that AgNPs could be toxic to plants such as aquatic *Lemna minor* (Gubbins et al. 2011) and terrestrial *Lolium multiflorum* (Yin et al. 2011) plants, microorganisms *Pseudomonas putida* (Fabrega et al. 2009), vertebrates such as zebrafish (Bowman et al. 2012; Asharani et al. 2008), and invertebrates *Caenorhabditis elegans* (Roh et al. 2009). For example, AgNPs appear to cause cell death

by disrupting bacterial cell membranes and increasing permeability, blocking Na^+ transport mechanisms and Na^+ homeostasis (Shahverdi et al. 2007). Other possible mechanism by which AgNPs may inactivate microorganisms include surface reactivity due to different crystal defects on nanomaterials surface (Pal et al. 2007).

In contrast, Ag^+ is known to interact with the thiol groups of the L-cysteine residue of certain proteins resulting in inactivation of their enzymatic functions (Feng et al. 2000), disruption of bacterial membrane integrity (Feng et al. 2000), increase in permeability, and likely affecting DNA replication (Neal 2008). Higher concentrations of Ag^+ interact with cytoplasmic components and nucleic acids (Feng et al. 2000).

Most of the available AgNPs have a core structure made of Ag^0 of varying size and shape and an organic coating with diverse functional groups. The coating prevents AgNPs aggregation by adsorption or covalent bonding of organic compounds that provide electrostatic, steric, or electrosteric repulsive forces between particles (Hotze et al. 2010; Levard et al. 2012). There are many different coatings used to stabilize AgNPs against aggregation including carboxylic acids, polymers, thiols, biological molecules, and surfactants (Tan et al. 2007). One of the most common carboxylic acids used as a capping agent is citrate; it has a comparatively small molecular weight and stabilizes AgNPs by increasing the magnitude of the negative surface charge (Tolaymat et al. 2010).

The objective of this study was to investigate the toxicity of equimolar silver nitrate and capped AgNPs solutions toward various microorganisms and to observe whether the toxicity is related to the physicochemical properties of AgNPs or is caused by the effects of dissolved Ag^+. Samples of bacteria, yeast, and algae were treated with citrate-capped AgNPs, 11-mercaptoundecanoic acid-capped AgNPs, or silver nitrate at equimolar doses rather than based on simply gravimetric weight. For the yeasts and bacteria, log reduction tests followed by zone of inhibition assays were conducted to emphasize the toxicity of silver. For the algae, the optical density was measured to quantify the number of surviving cells, and subsequently, the killing ability of the silver solutions. In addition, AFM imaging was performed to qualitatively show the effect of capped AgNPs and silver nitrate on the bacteria, yeast, and algae cells.

Materials and methods

Microorganisms and growth conditions

A panel of microorganisms belonging to various genera were tested in this study. The Gram-negative bacterium, *Pseudomonas aeruginosa* (ATCC 27317), found throughout the environment and the cause of numerous opportunistic infections in humans and the Gram-positive bacterium *Staphylococcus aureus* (ATCC 25923) commonly correlated with device-associated infections were analyzed in this research under identical conditions. The yeast *Saccharomyces cerevisiae,* the alga *Chlorella protothecoides,* and the unicellular flagellate *Euglena gracilis* were also used in the toxicity tests. The bacterial cultures were grown in Trypticase soy broth (TSB) (Difco, Sparks, MD) overnight (16 h) in 100 ml TSB with incubation at 37 °C under gyratory shaking (RPM × 120). The yeast *S. cerevisiae* was grown in 100 mL TSB (Difco, Sparks, MD) medium overnight (16 h) under gyratory shaking (RPM × 95) and cool-white fluorescent wide spectrum lamp (GRO-LUX, Osram Sylvania) that mimics natural sunlight (7600 lux) at room temperature. One milliliter of the bacterial and yeast suspensions obtained from overnight cultures was then transferred to 100 mL of fresh TSB and incubated 3–6 h at 37 °C for the bacteria and room temperature for the yeast to obtain approximately 10^{10} CFU of *P. aeruginosa*, 10^8 CFU of *S. aureus*, and 10^9 CFU of *S. cerevisiae* per mL. *C. protothecoides* inoculum was prepared by growing the algae in a phototrophic medium (Bristol's medium without $NaNO_3$) supplemented with 400 mg/L glycine. *E. gracilis* inoculum was prepared using a specific medium containing sodium acetate 1 g/L, beef extract 1 g/L, tryptone 2 g/L, yeast extract 2 g/L, and $CaCl_2*2H_2O$ 0.01 g/L. *C. protothecoides* and *E. gracilis* were grown under gyratory shaking (RPM × 95) and cool-white fluorescent wide spectrum lamp (GRO-LUX, Osram Sylvania) that mimics natural sunlight (7600 lux) at room temperature. When the optical density of the *C. protothecoides* and *E. gracilis* reached 0.4–0.5 at a wavelength of 610 nm, we proceeded with the toxicity experiments.

All reagents, unless otherwise specified, were obtained from Fisher Scientific. Materials and solutions were sterilized at 20 kPa and 121 °C.

Synthesis and characterization of silver nanoparticles

Citrate- and 11-mercaptoundecanoic acid-capped AgNPs were selected to test their specific effects on various microorganisms. Stock solutions of capped AgNPs in distilled water were provided by the Veinot' laboratory (University of Alberta, Department of Chemistry) and were stable at room temperature for months. The nanosilver and silver nitrate solutions were prepared by adding citrate-capped nanoparticles, 11-mercaptoundecanoic acid-capped nanoparticles, or silver nitrate to distilled water to achieve a 0.25 mM silver concentration.

Atomic force microscopy (AFM)

Applying AFM to image microbial surfaces requires an effective substrate that firmly attaches the cells while avoiding denaturation (Dorobantu et al. 2008). The microbial species employed in this study were strongly bound to the surface of glass slides coated with 3-aminopropyltrimethoxysilane (Genorama, Asper Biotech, Tartu, Estonia). 100 μL of the inoculum prepared with every microorganism was added to 900 μL of each of the nanosilver solutions, silver nitrate solution, PBS (untreated control) and incubated for 4 h. A droplet of each of the concentrated microbial suspensions was placed onto a silanized glass slide. After 60 min of settling, the microbial-coated glass was rinsed to remove loosely attached cells and transferred to the AFM stage to determine if structural changes occurred after exposure to the capped AgNPs or silver nitrate solutions. The AFM characterization was performed using a Molecular Force Probe 3D (MFP 3D) from Asylum Research (Santa Barbara, CA) controlled with IGOR PRO software (Wavemetrics, Portland, OR). Tapping mode AFM was used throughout the experiments with silicon nitride tips AC240TS (Olympus, nominal frequency of 50–90 kHz, nominal spring constant of 0.5–4.4 N/m).

Transmission electron microscopy (TEM)

The citrate and 11-mercaptoundecanoic acid-capped AgNPs were drop-cast from aqueous suspensions onto holey carbon–coated copper grids and dried under

vacuum. TEM was performed using a JEOL-2010 (LaB6 filament) electron microscope with an accelerating voltage of 200 keV. The diameters of the particles were determined by measuring the TEM images using the image processing and analyzing software ImageJ and histogram analysis was performed using Origin 8.0. The TEM experiments were performed in triplicate for each of the capped AgNPs.

Antimicrobial assays

Log reduction assay for P. aeruginosa, S. aureus, and S. cerevisiae

The log reduction assay determines the ability of AgNPs to kill a microbial inoculum and allows the computation of the rate of microbial killing. The procedure used in this study was similar to that described by Wright et al. (1998).

A phosphate-buffered saline (PBS) solution was prepared containing 8.5 g/L NaCl, 0.61 g/L KH_2PO_4 and 0.96 g/L K_2HPO_4, with a pH of 7. 100 µL of the bacteria or yeast inoculum was added to 900 µL of each of the nanosilver solutions, the silver nitrate solution, and PBS (untreated control). The samples were incubated for 30 min, 1, 2, or 4 h at 37 °C. In the meantime, a salt, polysorbate, sodium thioglycollate (SPS) solution was prepared, containing 0.85 % w/v NaCl, 1 % v/v polysorbate 20, and 0.1 % w/v sodium thioglycollate. After the samples were incubated for their corresponding time, 100 µL of each solution was added to 900 µL of SPS solution in order to inactivate the silver ions in solution. The samples were vortexed vigorously and serially diluted in PBS to achieve dilutions of 10^{-1} to 10^{-7}. Three 20 µL drops from each sample were plated on Trypticase soy agar (TSA) and incubated at 37 °C. The number of bacterial colonies in each sample was counted after 24 h in order to estimate the surviving number of colony forming units (CFU). The logarithm of the microorganisms in the original inoculants and in the exposed solutions was then determined. The log reductions were calculated as the difference between the log of the initial number of microorganisms and the log of the final surviving number of microorganisms. These experiments were performed in triplicate, and the results were the average of three independent experiments.

Toxicity assay for C. protothecoides and E. gracilis

600 µL of either citrate or mercaptoundecanoic acid-capped silver solution was added to 600 µL of algal suspension and 4.8 mL of growth medium for each alga and placed under gyratory shaking and fluorescent tubes at room temperature. 600 µL of distilled water was added to the controlled samples in place of the silver solution. The optical density of the samples was measured daily at 678 nm until the control samples reached an optical density of 0.5–0.6. The toxicity assay was performed in triplicate, and the results were the average of three independent experiments.

Zone of inhibition test

The zone of inhibition test measures microorganism susceptibility to an antimicrobial agent and shows microbial growth inhibition. The method used in this study, a modified form of the Kirby–Bauer test, is similar to that described by Wright et al. (1998). P. aeruginosa, S. aureus, and S. cerevisiae were incubated overnight as previously described in the log reduction assay. The test was performed in triplicate for all the silver samples employed in this study and for each microorganism tested. 1 mL of the inoculum obtained from these cultures was added to 100 mL of TSB and incubated at 37 °C for the bacteria and room temperature for the yeast for 3–6 h in order to obtain microbial cultures in the log phase of growth. Then, 100 µL of each microbial culture was added to TSA plates and spread over them. Silver dressing pieces, pre-moistened with 200 µL of sterile water, were prepared by impregnating 25.4 × 25.4 mm pieces of high-density polyethylene (HPDE) with 100 µL of each of the following solutions: silver nitrate, citrate-, and 11-mercaptoundecanoic acid-capped AgNPs and placed at the center of each plate. The plates were incubated overnight at 37 °C. The zone of inhibition was calculated by measuring the zone of microbial inhibition in each direction and measuring the width of the dressing itself. The dressing width was subtracted from the zone width and an average of the results from each direction was calculated as the overall zone of inhibition.

Results

Transmission electron microscopy (TEM)

Figure S1 in SI presents a TEM image of the citrate-capped AgNPs (a) along with the particle size distribution (b). Figure S2 displays a TEM image of the 11-mercaptoundecanoic acid-capped AgNPs accompanied by the particle size distribution (b). We notice that the citrate-capped AgNPs tend to be agglomerated on the TEM substrates and the singles have a diameter d = 17.5 ± 9.4 nm. The 11-mercaptoundecanoic acid-capped AgNPs do not agglomerate as a result of drying during TEM sample preparation and have a diameter d = 38.8 ± 3.6 nm.

Atomic force microscopy (AFM)

Figure S3 in SI shows AFM amplitude images of the citrate-capped AgNPs (a) and 11-mercaptoundecanoic acid-capped AgNPs (b). Consistent with the TEM analysis, the AFM image in Fig. S3 (a) clearly shows the existence of single dispersed citrate-capped AgNPs sized in the range of ca. 20–30 nm together with aggregates of several hundred nms. In contrast, 11-mercaptoundecanoic acid-capped AgNPs appear only as individuals [Fig. S3 (b)] sized in the range of ca. 30–40 nm.

Microbicidal efficacy of silver nanoparticles

Log reduction assay

Figure 1 shows log reduction results for *P. aeruginosa, S. aureus*, and *S. cerevisiae* treated with 11-mercaptoundecanoic acid-capped AgNPs, citrate-capped AgNPs, or silver nitrate for 0.5, 1, 2, and 4 h. A log reduction of three or greater is considered to be microbicidal after 30 min of exposure. In the case of *P. aeruginosa* (Fig. 1a), 11-mercaptoundecanoic acid-capped AgNPs became bactericidal after 2 h of exposure, with a maximum log reduction of 3.73 at 4 h. The treatment with citrate-capped AgNPs was not bactericidal resulting in a maximum log reduction of 0.685 at 4 h. In contrast, the treatment with silver nitrate was bactericidal at all exposure times resulting in a maximum log reduction of 4.93 after 30 min of exposure. However, for *S. aureus* (Fig. 1b), no bactericidal activity was observed with any of the
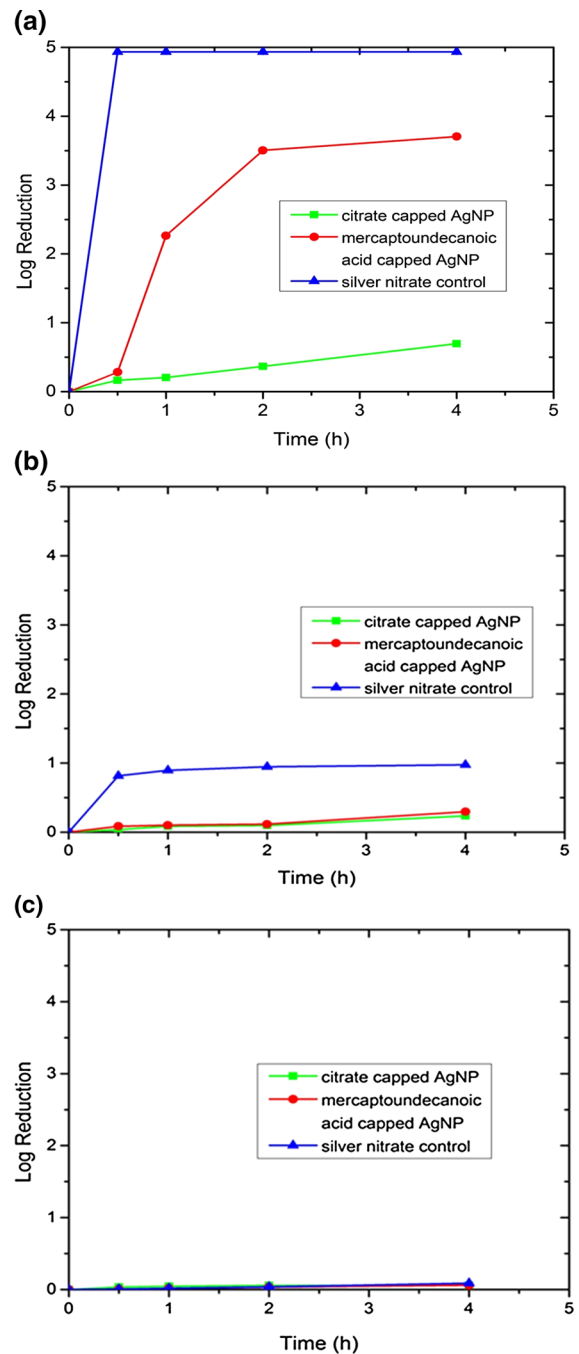

Fig. 1 Log reduction for *P. aeruginosa* (**a**), *S. aureus* (**b**), and *S. cerevisiae* (**c**) cells after 0.5, 1, 2, and 4 h of treatment with 11-mercaptoundecanoic acid-capped AgNPs, citrate-capped AgNPs, or silver nitrate

capped AgNPs. The treatment with silver nitrate resulted in a maximum log reduction of 1.08 at 4 h. None of the silver treatments was significantly toxic to

the yeasts (Fig. 1c). Treatment with 11-mercaptoundecanoic acid-capped AgNPs resulted in a maximum log reduction of 0.029 at 4 h. Treatment with citrate-capped AgNPs resulted in a maximum log reduction of 0.025 at 4 h and treatment with silver nitrate resulted in a maximum log reduction of 0.056 at 4 h.

Figure 2 displays the optical density results for *C. protothecoides* and *E. gracilis* cells under control conditions and during treatment with 11-mercaptoundecanoic acid-capped AgNPs, citrate-capped AgNPs, or silver nitrate, after 0, 24, and 48 h of exposure. The results suggest that silver nitrate had the most toxic effect on these cells, followed by the 11-mercaptoundecanoic acid-capped AgNPs, which were slightly toxic, and the citrate-capped AgNPs, which were negligibly toxic.
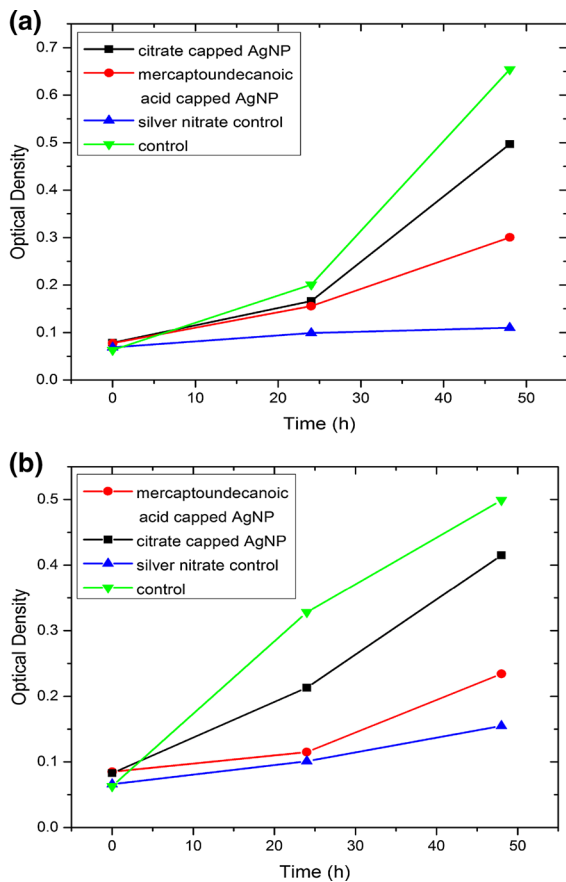
Fig. 2 Optical density of *C. protothecoides* (**a**) and *E. gracilis* (**b**) cells under control conditions or during treatment with 11-mercaptoundecanoic acid-capped AgNPs, citrate-capped AgNPs, or silver nitrate

Zone of inhibition assay

Table S1 in SI summarizes the results of the zone of inhibition test for *S. aureus, P. aeruginosa,* and *S. cerevisiae*. We observe that citrate-capped AgNPs do not produce a zone of inhibition to any of the three microorganisms tested. However, silver nitrate produces a 2 mm zone of inhibition against *S. aureus* and 4 mm zone of inhibition against *P. aeruginosa*. As observed in Table S1, the mercaptoundecanoic acid-capped AgNPs present a 2-mm zone of inhibition against *P. aeruginosa*. None of the silver treatments presents a zone of inhibition against the yeast *S. cerevisiae*. The zones of inhibition results are reproducible during the three repeats for each microorganism.

AFM of microbial cells

The morphological damage induced by the microorganism's exposure to the capped AgNPs and silver nitrate was studied by AFM.
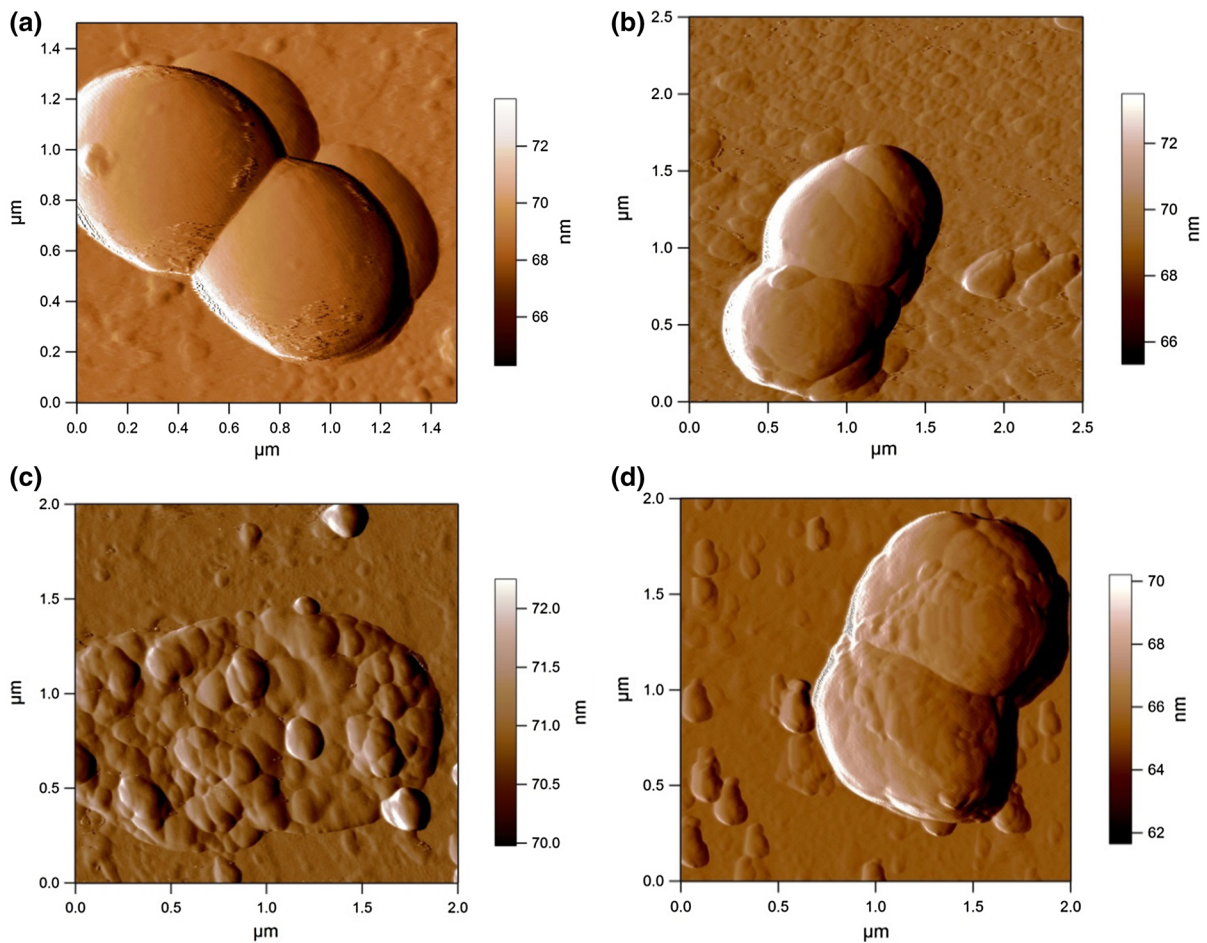
Figure 3 emphasizes the morphology of *P. aeruginosa* before (a) and after being in contact with citrate-capped AgNPs (b), 11-mercaptoundecanoic acid-capped AgNPs (c), and silver nitrate (d) for 4 h. All these figures reveal intact cells featuring undamaged membranes. It is interesting to note the vast number of 11-mercaptoundecanoic acid-capped AgNPs present on the surface of *P. aeruginosa* (Fig. 3c). In contrast, only a small number of citrate-capped AgNPs are detected on the surface of *P. aeruginosa*.

Figure 4 shows *S. aureus* before (a) and after being in contact with citrate-capped AgNPs (b), 11-mercaptoundecanoic acid-capped AgNPs (c), and silver nitrate (d) for 4 h. Similar to *P. aeruginosa,* these cells do not appear to be traumatized by the treatment with any of the AgNPs or silver nitrate and resemble to the control image in Fig. 4a.

Figure 5 shows *S. cerevisiae* before (a) and after treatment with citrate-capped AgNPs (b), 11-mercaptoundecanoic acid-capped AgNPs (c), or silver nitrate (d) for 4 h.

Similar to the bacterial species, the yeast cells do not seem to be distressed under the presence of either nanoparticles or silver nitrate. They look similar to the control conditions shown in Fig. 5a.

Figure 6 shows *C. protothecoides* before (a) and after treatment with (b) citrate-capped AgNPs, (c) 11-mercaptoundecanoic acid-capped AgNPs,

Fig. 3 Representative AFM images of *P. aeruginosa* before (**a**) and after treatment with citrate-capped AgNPs (**b**), 11-mercaptoundecanoic acid-capped AgNPs (**c**), or silver nitrate (**d**) for 4 h

(d) silver nitrate for 4 h. Although none of the nanoparticles affected the cellular membrane of *C. protothecoides,* silver nitrate treatment disrupted the algal membrane (Fig. 6d). The intracellular material has leaked out of the cell and its surface was irregular, with large zones of depression. The volume of the cells was considerably depressed, with respect to the control sample.

Figure 7 shows *E. gracilis* before (a) and after treatment with citrate-capped AgNPs (b), 11-mercaptoundecanoic acid-capped AgNPs (c), or silver nitrate (d) for 4 h.

AFM images of *E. gracilis* cells in Fig. 7 reveal that the cell morphology changed due to the stress induced by the AgNPs and AgNO₃. It can be observed that the shapes of the cells altered from spindle (Fig. 7a) to round (Fig. 7b–d) with the cells exhibiting

an increase in diameter. Damage to the cell membrane was observed in the presence of AgNPs (Fig. 7d).

Discussion

This study investigates the comparative toxicity effects of equimolar solutions of citrate and 11-mer-captoundecanoic acid-capped AgNPs, and silver nitrate on bacteria, yeast, and algae and explores which form of silver is more effective to intentionally fight the undesirable growth of these microorganisms.

The log reduction results in Fig. 1 show that silver nitrate is a more potent killer of both Gram-positive and Gram-negative bacteria than either type of AgNPs when compared at a similar molar concentration. In
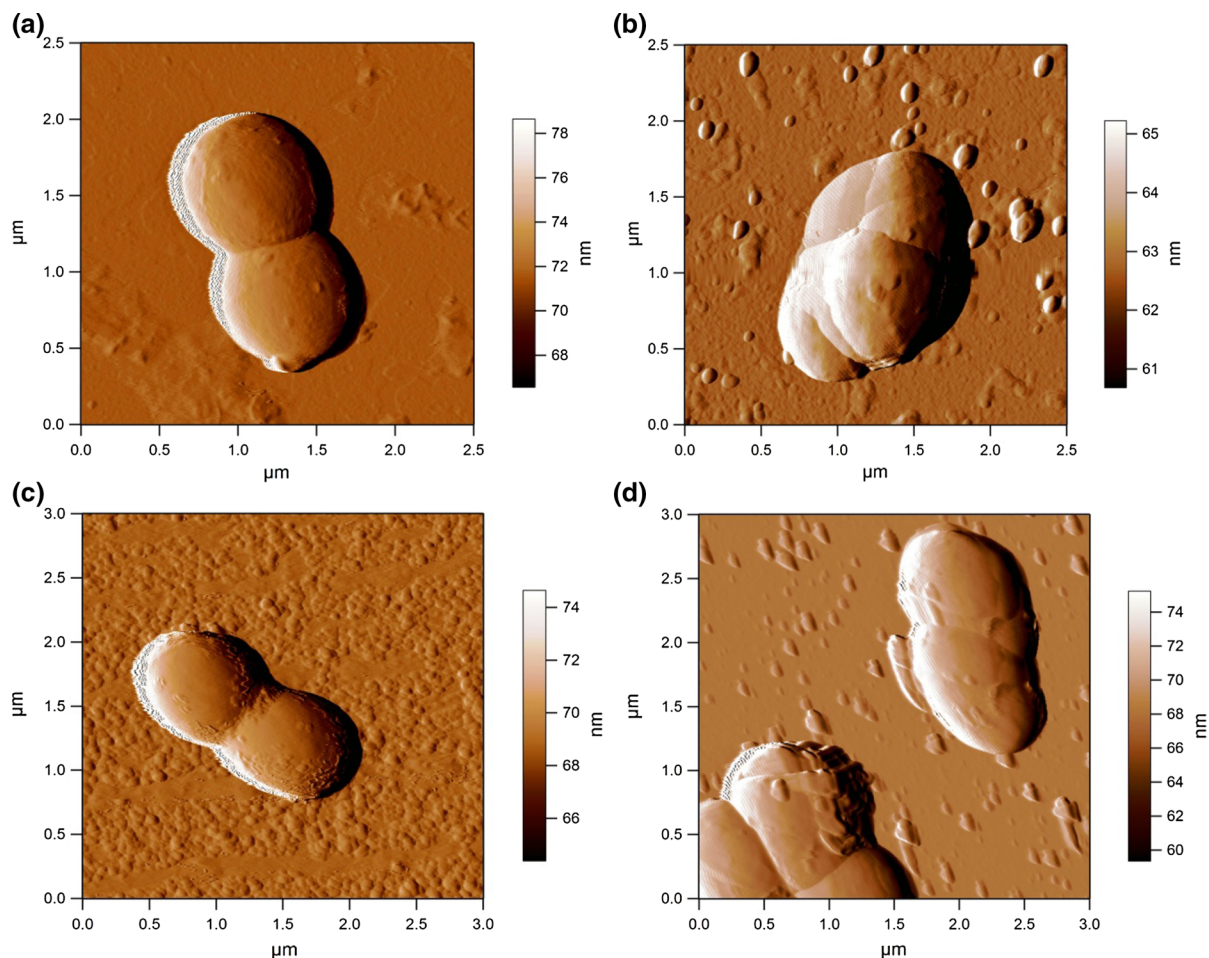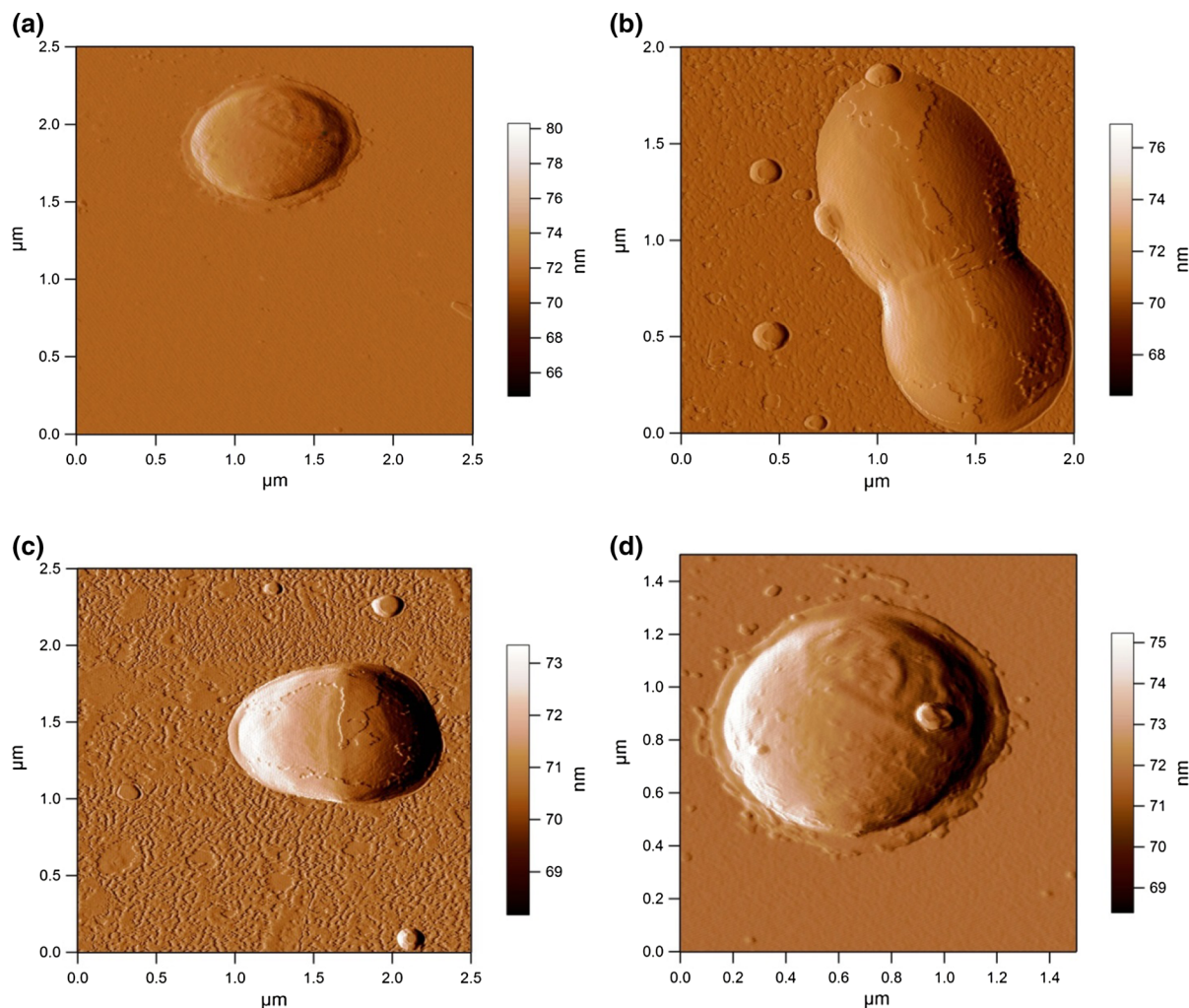
Fig. 4 Representative AFM images of the Gram-positive *S. aureus* before (**a**) and after treatment with citrate-capped AgNPs (**b**), 11-mercaptoundecanoic acid-capped AgNPs (**c**), or silver nitrate (**d**) for 4 h

addition, the algal cells *C. protothecoides* and *E. gracilis* present higher susceptibility to silver nitrate than to any of the capped AgNPs as emphasized by the optical density results in Fig. 2. The log reduction and optical density results prove that the antimicrobial activity of AgNPs is dictated primarily by the Ag^+ ions released from their surface. Our results are consistent with the work of Navarro et al. who presented evidence that AgNPs toxicity to *Chlamydomonas reinhardtii* algae is mainly the result of Ag^+ dissolution and that nanosilver serves primarily as a source of dissolved Ag^+ ions (Navarro et al. 2008). Miao et al.(2009) also showed that dissolved Ag^+ ions dictate nanosilver toxicity toward algal cells. Xiu et al. (2012) studied the effect of various AgNPs (PEG- or PVP-coated, of three different sizes each) on *E. coli* and concluded that Ag^+

is the definitive molecular toxicant. They ruled out direct particle-specific biological effects by showing the lack of toxicity of AgNPs when synthesized and tested under strictly anaerobic conditions that precluded Ag^0 oxidation and Ag^+ release.

It is interesting to note that *P. aeruginosa* suffered a greater log reduction than *S. aureus* in the presence of 11-mercaptoundecanoic acid-capped AgNPs suggesting that some species are more sensitive to silver than others. The higher susceptibility of *P. aeruginosa* to Ag^+ than *S. aureus* could be explained in terms of the differences in their wall structures While the Gram-positive *S. aureus* possess a thick, rigid cell wall made up of peptidoglycan and teichoic acids, the Gram-negative *P. aeruginosa* have a thin peptidoglycan layer that can be easier penetrated by Ag^+ (Marcus et al. 2012).
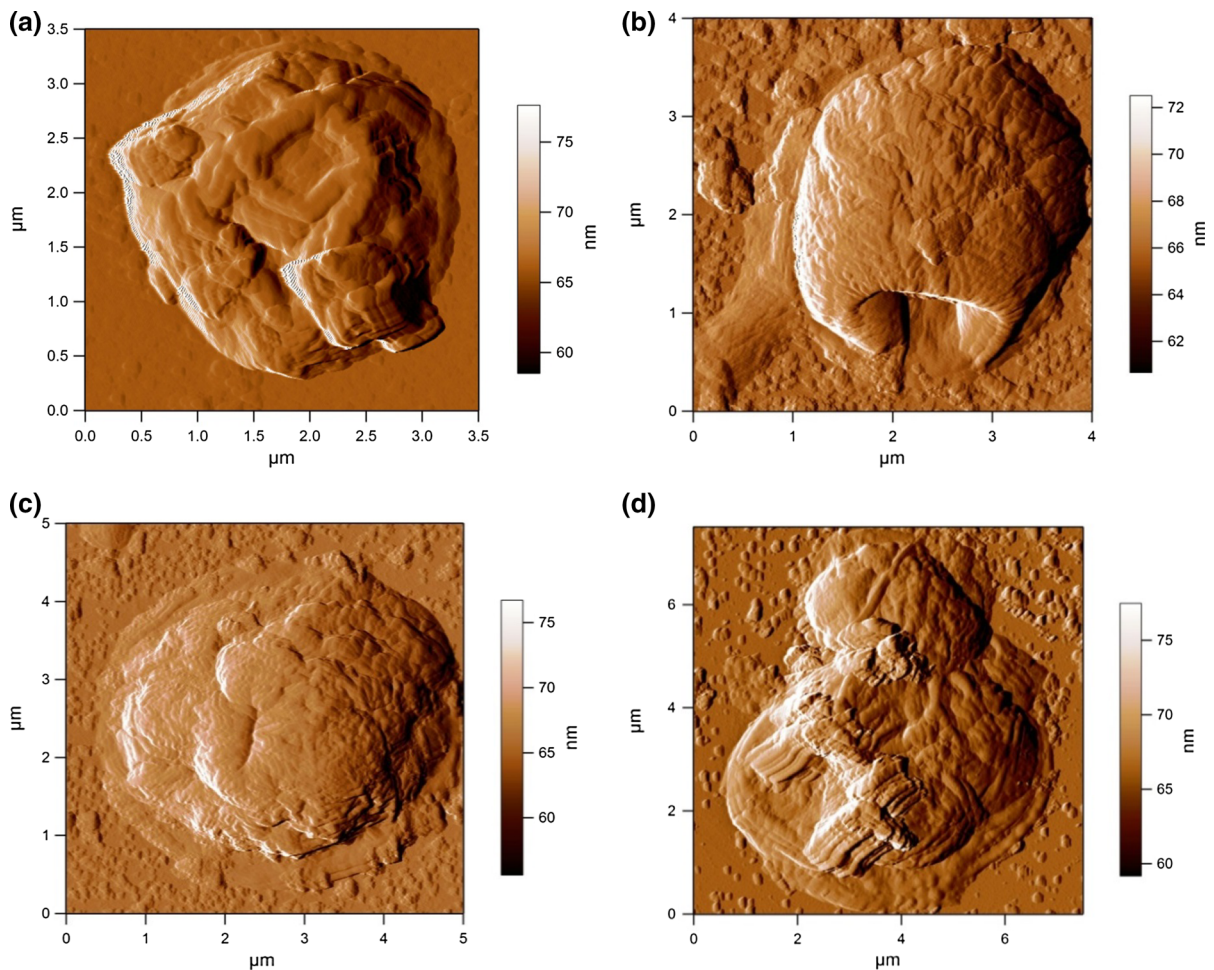
Fig. 5 Representative AFM images of the yeast *S. cerevisiae* before (**a**) and after treatment with citrate-capped AgNPs (**b**), 11-mercaptoundecanoic acid-capped AgNPs (**c**), or silver nitrate (**d**) for 4 h

When comparing the toxicity effects of the two capped AgNPs, the 11-mercaptoundecanoic acid-capped AgNPs seem to be more harmful than citrate-capped AgNPs (Figs. 1 and 2) suggesting that the capping agent has a significant effect on the toxicity of nanoparticles. Pace et al. (2010) investigated the toxicity of polyethylene oxide and 11-mercaptoundecanoic acid-coated CdSe/ZnS quantum dots to *Daphnia magna* after 48 h of exposure. Their results show that the coating on nanoparticles has significant impact on short-term toxicity. The 11-mercaptoundecanoic acid quantum dots were more toxic to *Daphnia magna* and allowed Cd^{2+} to go in the solution. Consequently, the emergence of dissolved Cd^{2+} in solution indicates that the

11-mercaptoundecanoic acid coating is not stable. The importance of AgNPs surface coating toward the freshwater cladoceran *Daphnia magna* was investigated by Zhao and Wang (2012) who used lactate-, polyvinylpyrrolidone-, and sodium dodecylbenzene sulfonate-capped AgNPs. They concluded that the surface coatings influenced the dissolution of AgNPs into soluble Ag, resulting in the different toxicities of AgNP to *Daphnia magna*.

According to Liu and Hurt (2010), AgNPs undergo oxidization in aqueous solutions exposed to air resulting in the release of Ag^+ under acidic conditions:

$$4Ag^0 + O_2 = 2Ag_2O \qquad (1)$$

Fig. 6 Representative AFM images of *C. protothecoides* before (**a**) and after treatment with citrate-capped AgNPs (**b**), 11-mercaptoundecanoic acid-capped AgNPs (**c**), or silver nitrate (**d**) for 4 h

$$2Ag_2O + 4H^+ = 4Ag^+ + 2H_2O \qquad (2)$$
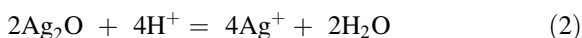
The microbicidal tests conducted in this study show that 11-mercaptoundecanoic acid capping does not protect AgNPs from the reactions (1) and (2) and the Ag$^+$ released from the nanoparticles is almost as effective killer as the silver nitrate solution. Contrary, the citrate coating acts as a chemical barrier and it is able to reduce the outgoing silver (Kittler et al. 2010). According to Liu and Hurt (2010), some surface coatings have been observed to eliminate nanoparticles toxicity to various organisms, from bacteria to human skin keratinocytes due to the reduction of NPs dissolution.

The zone of inhibition results in Table S1 show that silver nitrate created a zone of 4 mm in diameter with *P.*

aeruginosa while the 11-mercaptoundecanoic acid-capped AgNPs generated a zone of 2 mm. This result suggests that 11-mercaptoundecanoic acid-capped AgNPs present a similar toxicity to silver nitrate which is in discordance with the log reduction results that show that silver nitrate is 4 1/2 orders of magnitude more toxic than the 11-mercaptoundecanoic acid-capped AgNPs. The zone of inhibition test was included in this study to show the qualitative difference between the toxicity of citrate-capped silver nanoparticles and 11-mercaptoundecanoic acid-capped AgNPs; the former released virtually no silver with biological activity.

In the case of *S. cerevisiae*, the log reduction results are not significantly different, indicating no difference in toxicity for the various forms of silver with respect to the yeast (Fig. 1c). The yeast *S. cerevisiae* wall is
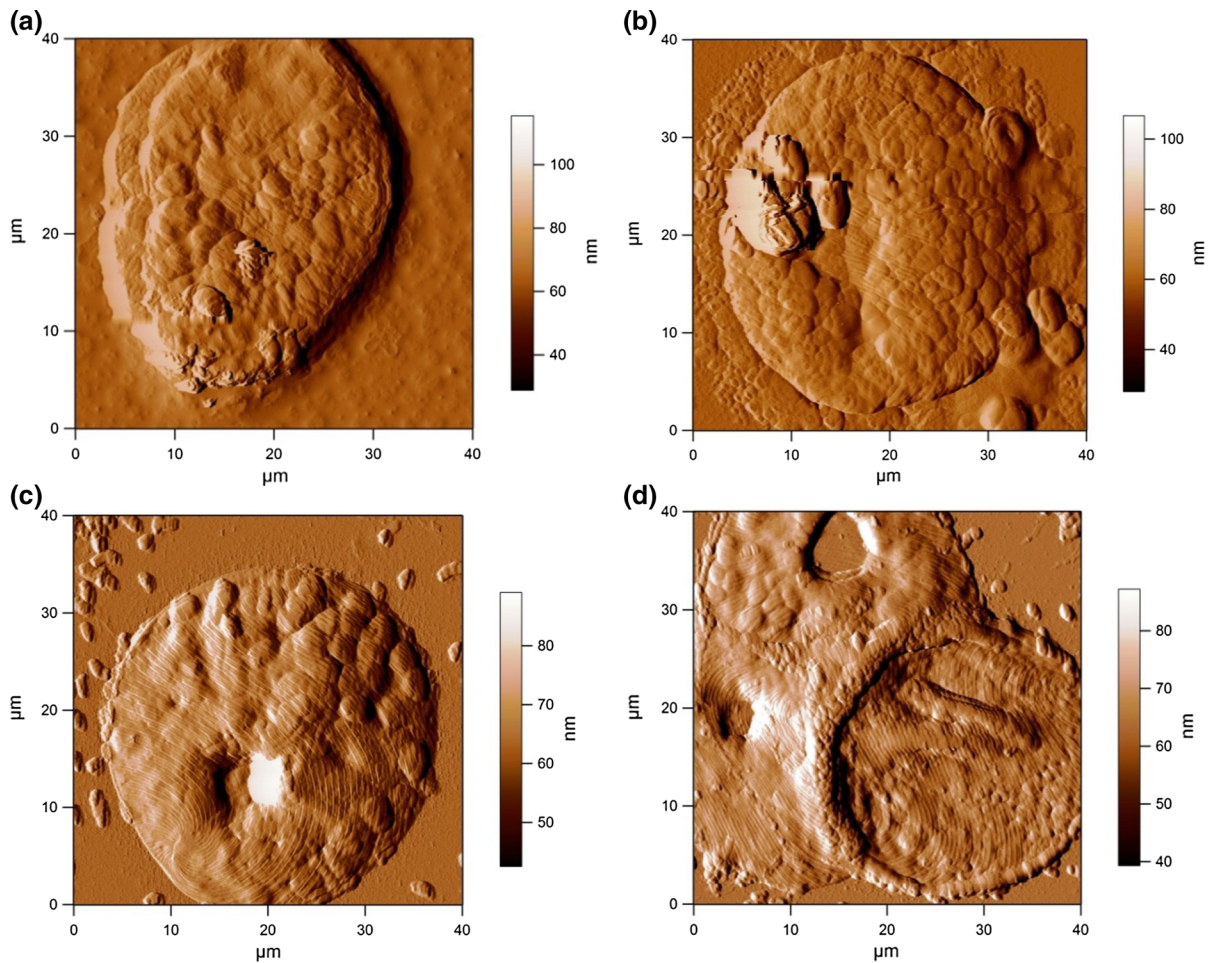
Fig. 7 Representative AFM images of *E. gracilis* before (**a**) and after treatment with citrate-capped AgNPs (**b**), 11-mercaptounde-canoic acid-capped AgNPs (**c**), or silver nitrate (**d**) for 4 h

composed of an inner layer of polysaccharides namely β-glucans, chitin, and an outer layer of mannoproteins that extend into the medium. This cell wall structure seems to withstand the toxicity of Ag^+ (Madigan et al. 2012).

The AFM images in Figs. 3, 4 and 5 show that *P. aeruginosa, S. aureus,* and *S. cerevisiae* cells do not appear to be traumatized under the presence of either AgNPs or silver nitrate; the cells look as they do under the control conditions. In contrast, the algal cells *C. protothecoides* and *E. gracilis* lyse and collapse (Figs. 6d, 7d) following addition of silver nitrate, further confirming that Ag^+ displayed higher toxicity than AgNPs.

The functional groups on nanoparticle surfaces play a very important role in regards to their interactions at the

cell surface. They decide the potential interactions such as, van der Waals, hydration or hydrophobic forces, electrostatic or specific interactions (hydrogen bonding, receptor-ligand interactions) that can take place at the cell/nanoparticles interface (Ma and Lin 2013).

In this study, the use of sodium citrate or 11-mercaptoundecanoic acid as capping agents generates negatively charged AgNPs and also confer them a hydrophilic surface. As most microbial cells possess a negative charge, we can explain the lack of adherence of citrate-capped AgNPs on *P. aeruginosa, S. aureus, S. cerevisiae, E. gracilis,* and *C. protothecoides* surfaces (Figs. 3, 4, 5, 6, 7b) by the electrostatic repulsive forces that develop between the two negatively charged surfaces. However, we notice an agglomeration of 11-mercaptoundecanoic acid-

capped AgNPs on *P.aeruginosa* (Fig. 3c) which is known to possess a hydrophilic surface (Sondi and Salopek-Sondi 2004). We would expect that the electrostatic repulsive force in combination with the repulsive hydration forces between the two hydrophilic surfaces to limit the adherence of 11-mercaptoundecanoic acid-capped AgNPs on *P. aeruginosa* surface. However, the presence of adhered 11-mercaptoundecanoic acid-capped AgNPs on *P. aeruginosa* surface suggest that additional specific interactions are involved. The proximity of the 11-mercaptoundecanoic acid-capped AgNPs to the *P. aeruginosa* surface facilitates the uptake of Ag^+ inside the cell and increases its toxicity toward this microorganism.

In spite of the slight difference in the cell wall composition and conformation of bacteria, yeast, and algae, the tough cell walls of these microorganisms can play a protective role in supporting the cell structure and resisting the harmful effect of AgNPs. However, Ag^+ that dissolves from the nanoparticles surface exhibits a toxic effect which is not dependent on the particle size but on the coating used. Although, both capped AgNPs employed in this study had similar dimensions, the citrate-capped AgNPs produced no significant killings when compared to the 11-mercaptoundecanoic acid-capped AgNPs. This observation reinforces our findings that AgNPs do not present any specific effect on the toxicity of the studied microorganisms and this is in accordance with the work of Monteiro et al. (2012).

Conclusion

In this study, we demonstrated that capped AgNPs were less effective in suppressing the growth of bacteria, yeast, and algae than equimolar silver nitrate solutions prepared with the same concentration of silver. Notably, the group of microorganisms most affected by the Ag^+ was algae followed by bacteria. Although some species were more susceptible to silver than others, none of the silver nitrate, 11-mercaptoundecanoic acid-capped silver nanoparticle, or citrate-capped silver nanoparticle had a significant toxic effect on the yeast.

The 11-mercaptoundecanoic acid-capped AgNPs were consistently more toxic than citrate-capped silver nanoparticles emphasizing that the organic layer on the nanoparticles controls their surface properties. While the citrate coating acts as a chemical barrier and it is able to reduce the outgoing silver, the 11-mercaptoundecanoic acid capping agent is not very stable and allows the Ag^+ ions to be released into the medium suggesting that the microbicidal action of the capped AgNPs is dependent on the amounts of ions released from their surface.

The AFM images showed that the capped AgNPs did not damage any of the microbes employed in this study; the cells appeared similar to the controls. However, silver nitrate disrupted the algal cell membranes. This observation reinforces the hypothesis that only the dissolved silver ions are responsible for the biological action specifically pronounced against microorganisms.

In conclusion, the antimicrobial activity of AgNPs is dictated by Ag^+ ions alone and could be controlled by modulating Ag^+ released based on the type of coating used. The antimicrobial activity of nanosilver could be exploited to prevent microbial colonization of medical devices.

References

Asharani PV, Wu YL, Gong Z, Valiyaveettil S (2008) Toxicity of silver nanoparticles in zebrafish models. Nanotechnology 19:255102

Bowman CR, Bailey FC, Elrod-Erickson M, Neigh AM, Otter RR (2012) Effects of silver nanoparticles on zebrafish (*Danio rerio*) and *Escherichia coli* (ATCC 25922): a comparison of toxicity based on total surface area versus mass concentration of particles in a model eukaryotic and prokaryotic system. Environ Toxicol Chem 31:1793–1800

Dorobantu LD, Bhattacharjee S, Foght JM, Gray MR (2008) Atomic force microscopy measurement of heterogeneity in bacterial surface hydrophobicity. Langmuir 24:4944–4951

Fabrega J, Renshaw JC, Lead JR (2009) Interactions of silver nanoparticles with *Pseudomonas putida* biofilms. Environ Sci Technol 43:9004–9009

Feng Q, Wu J, Chen G, Cui F, Kim T, Kim J (2000) A mechanistic study of the antibacterial effect of silver ions on *Escherichia coli* and *Staphylococcus aureus*. J Biomed Mater Res 52:662–668

Fubini B, Fenoglio I, Tomatis M, Turci F (2011) Effect of chemical composition and state of the surface on the toxic response to high aspect ratio nanomaterials. Nanomedicine 6:899–920

Gubbins EJ, Batty LC, Lead JR (2011) Phytotoxicity of silver nanoparticles to *Lemna minor*. Environ Pollut 159:1551–1559

Hotze EM, Phenrat T, Lowry GV (2010) Nanoparticle aggregation: challenges to understanding transport and reactivity in the environment. J Environ Qual 39:1909–1924

Kittler S, Greulich C, Diendorf J, Koeller M, Epple M (2010) Toxicity of silver nanoparticles increases during storage because of slow dissolution under release of silver ions. Chem Mater 22:4548–4554

Levard C, Hotze EM, Lowry GV, Brown GE Jr (2012) Environmental transformations of silver nanoparticles: impact on stability and toxicity. Environ Sci Technol 46:6900–6914

Liu J, Hurt RH (2010) Ion release kinetics and particle persistence in aqueous nano-silver colloids. Environ Sci Technol 44:2169–2175

Ma S, Lin D (2013) The biophysicochemical interactions at the interfaces between nanoparticles and aquatic organisms: adsorption and internalization. Environ Sci Process Impacts 15:145–160

MacCormack TJ, Goss GG (2008) Identifying and predicting biological risks associated with manufactured nanoparticles in aquatic ecosystems. J Ind Ecol 12:286–296

Madigan MT, Martinko JM, Bender K, Buckley DP, Stahl DA (2012) Brock biology of microorganisms, 12th edn. Pearson/Benjamin Cummings, San Francisco

Marcus IM, Herzberg M, Walker SL, Freger V (2012) *Pseudomonas aeruginosa* attachment on QCM-D sensors: the role of cell and surface hydrophobicities. Langmuir 28:6396–6402

Martinez-Gutierrez F, Thi EP, Silverman JM, de Oliveira CC, Svensson SL, Hoek AV, Sanchez EM, Reiner NE, Gaynor EC, Pryzdial ELG, Conway EM, Orrantia E, Ruiz F, Av-Gay Y, Bach H (2012) Antibacterial activity, inflammatory response, coagulation and cytotoxicity effects of silver nanoparticles. Nanomedicine 8:328–336

Maurer-Jones MA, Gunsolus IL, Murphy CJ, Haynes CL (2013) Toxicity of engineered nanoparticles in the environment. Anal Chem 85:3036–3049

Miao AJ, Schwehr KA, Xu C, Zhang SJ, Luo ZP, Quigg A, Santschi PH (2009) The algal toxicity of silver engineered nanoparticles and detoxification by exopolymeric substances. Environ Pollut 157:3034–3041

Monteiro DR, Silva S, Negri M, Gorup LF, de Camargo ER, Oliveira R, Barbosa DB, Henriques M (2012) Silver nanoparticles: influence of stabilizing agent and diameter on antifungal activity against *Candida albicans* and *Candida glabrata* biofilms. Lett Appl Microbiol 54:383–391

Navarro E, Piccapietra F, Wagner B, Marconi F, Kaegi R, Odzak N, Sigg L, Behra R (2008) Toxicity of silver nanoparticles to *Chlamydomonas Reinhardtii*. Environ Sci Technol 42:8959–8964

Neal AL (2008) What can be inferred from bacterium-nanoparticle interactions about the potential consequences of environmental exposure to nanoparticles? Ecotoxicology 17:362–371

Nel A, Xia T, Madler L, Li N (2006) Toxic potential of materials at the nanolevel. Science 311:622–627

Pace HE, Lesher EK, Ranville JF (2010) Influence of stability on the acute toxicity of CdSe/ZnS nanocrystals to *Daphnia Magna*. Environ Toxicol Chem 29:1338–1344

Pal S, Tak YK, Song JM (2007) Does the antibacterial activity of silver nanoparticles depend on the shape of the nanoparticle? A study of the gram-negative bacterium *Escherichia coli*. Appl Environ Microbiol 73:1712–1720

Roh J, Sim SJ, Yi J, Park K, Chung KH, Ryu D, Choi J (2009) Ecotoxicity of silver nanoparticles on the soil nematode *Caenorhabditis elegans* using functional ecotoxicogenomics. Environ Sci Technol 43:3933–3940

Schacht VJ, Neumann LV, Sandhi SK, Chen L, Henning T, Klar PJ, Theophel K, Schnell S, Bunge M (2013) Effects of silver nanoparticles on microbial growth dynamics. J Appl Microbiol 114:25–35

Shahverdi AR, Fakhimi A, Shahverdi HR, Minaian S (2007) Synthesis and effect of silver nanoparticles on the antibacterial activity of different antibiotics against *Staphylococcus aureus* and *Escherichia coli*. Nanomedicine 3:168–171

Sondi I, Salopek-Sondi B (2004) Silver nanoparticles as antimicrobial agent: a case study on *E. coli* as a model for gram-negative bacteria. J Colloid Interface Sci 275:177–182

Tan S, Erol M, Attygalle A, Du H, Sukhishvili S (2007) Synthesis of positively charged silver nanoparticles via photoreduction of $AgNO_3$ in branched polyethyleneimine/HEPES solutions. Langmuir 23:9836–9843

Tolaymat TM, El Badawy AM, Genaidy A, Scheckel KG, Luxton TP, Suidan M (2010) An evidence-based environmental perspective of manufactured silver nanoparticle in syntheses and applications: a systematic review and critical appraisal of peer-reviewed scientific papers. Sci Total Environ 408:999–1006

Wright JB, Hansen DL, Burrell RE (1998) The comparative efficacy of two antimicrobial barrier dressings: in-vitro examination of two controlled release of silver dressings. Wounds 10:179–188

Xiu Z, Zhang Q, Puppala HL, Colvin VL, Alvarez PJJ (2012) Negligible particle-specific antibacterial activity of silver nanoparticles. Nano Lett 12:4271–4275

Yin L, Cheng Y, Espinasse B, Colman BP, Auffan M, Wiesner M, Rose J, Liu J, Bernhardt ES (2011) More than the ions: the effects of silver nanoparticles on *Lolium multiflorum*. Environ Sci Technol 45:2360–2367

Zhao CM, Wang WX (2012) Importance of surface coatings and soluble silver in silver nanoparticles toxicity to *Daphnia magna*. Nanotoxicology 6:361–370